Desalination and Water Treatment
www.deswater.com

doi:10.5004/dwt.2019.24463

164 (2019) 62–74
October

Effect of graphene oxide on desalination performance of cellulose acetate mixed matrix membrane

Amin Shams[a,*], Seyyed Ahmad Mirbagheri[a], Yousef Jahani[b]

[a]*Department of Civil and Environmental Engineering, K.N. Toosi University of Technology, No. 1346, Vali Asr street, Mirdamad Intersection Tehran, Iran, Tel. +98(21)88779474, Fax +98(21)88779476, email: amin.shams@mail.kntu.ac.ir (A. Shams), mirbagheri@kntu.ac.ir (S.A. Mirbagheri)*
[b]*Department of Plastics, Faculty of Processing, Iran Polymer and Petrochemical Institute, Pajoohesh Blvd, District 22, Tehran, Iran, Tel. +98(21), email: y.jahani@ippi.ac.ir (Y. Jahani)*

Received 9 December 2018; Accepted 23 May 2019

ABSTRACT

In this study, the effect of different amounts of graphene oxide (GO) nanoparticles on the desalination performance of cellulose acetate (CA) reverse osmosis mixed matrix membranes has been investigated. To investigate the interactions between different parameters and optimize the membrane performances, response surface methodology (RSM) was applied. For a simultaneous enhancement of salt rejection and water flux performances, the analysis by central composite design (CCD) suggested the optimum values of 0.009 wt.% for GO content, 3500 ppm for feed salinity, and 18 bar for applied pressure as significant factors. The membrane, prepared and tested based on the optimal values, was found to have 11.12 l/m^2·h permeation flux and 58.08% salt rejection which were in good agreement with the predicted values of 11.42 l/m^2·h and 59.53%. It has been revealed that optimization using CCD in the range of the applied experimental parameters is a reliable method for prediction of the CA/GO membranes performance.

Keywords: Graphene oxide; Cellulose acetate; Mixed matrix membrane; Desalination; Response surface methodology; Central composite design

1. Introduction

In recent years, considerable efforts have been put on obtaining fresh water from saline sea water as a most readily available source of water. Two dominant factors in membrane filtration technique are ease of use and energy saving, which have caused this technique to be more popular compared to other conventional methods [1].

Different types of polymers have been used as membrane materials for desalination applications: polyamide (PA), polyvinylidene difluoride (PVDF), polyethersulfone (PES), and cellulose acetate. Choosing the type of polymer for separation process is not a trivial task. Cellulose acetate (CA) is an environmental polymer which is obtained from sustainable and renewable sources. CA-based membranes are suitable for applications requiring high flux capacity [2–5], high durability, more hydrophilicity and low fouling potential [6]. Its low price and good resistance against chlorine agents have made it one of the most utilized polymers. Many studies have been carried out to improve the properties of CA membranes. One of the best ways to enhance the performance of these membranes is to change their morphology through adding different additives to the base polymer structure. In this regard, mixed matrix membranes (MMMs) are considered as a new technology composed of a base polymer and inorganic particles that are distributed homogeneously and uniformly in the polymer matrix. These membranes have shown remarkable improvements in the separation of gases [7] and in desalination applications [8]. Various inorganic particles, such as titanium dioxide [9], silicon dioxide (SiO_2) [10], polyhedral oligomeric silsesquioxane (POSS) [11], and

*Corresponding author.

multi-walled carbon nanotubes (MWCNT) [12–14], have been investigated for use in desalination membranes.

CA/SiO_2 nanocomposite membrane which has been used for removing $MgSO_4$ salt from aqueous solutions can enhance the salt rejection with lower water flux compared to pristine CA membrane, due to morphology changes [10]. The effect of different CA and CNTs concentrations on membrane performance and permeation flux through membrane has also been investigated and the optimum polymer/solvent ratio of 25:75, which is acceptable for desalination applications, has been reported [12]. In another research, the effect of the presence of functionalized CNTs on the morphology and performance of CNT/CA membranes containing 0.0005, 0.005 and 0.01 wt.% CNT was studied. The use of dead-end desalination pilot plant with 1000 ppm NaCl at 24 atm applied pressure showed 54% improvement in permeation rates as well as 6% reduction in salt retention, in the samples containing 0.0005wt.% CNT [13]. The CA composite membranes with POSS prepared by phase inversion method was the subject of another study [11], in which dispersion, compaction and flux properties were studied. Graphene oxide as a nanomaterial is widely used in various studies due to its intrinsic properties, extraordinary surface area, high mechanical strength, hydrophilic functional groups, and excellent dispersibility in many polymer matrices [15] PVDF/GO composites are usually studied [16] as a candidate for ultra filtration membranes, and it was found that, in comparison with their pristine counterpart, the properties, structure, and performance of membrane were obviously improved by 0.2 wt.% of GO. The influences of GO on the performance and anti-fouling properties of PES/GO mixed matrix membrane fabricated via phase inversion method are investigated. Higher dye removal capacity and water flux, the best anti-biofouling property and the highest mean pore radius and porosity were achieved by adding 0.5 wt.% of GO [17]. The performance of PES/GO nanocomposite membranes was evaluated [18] and found that 2000 ppm GO loading led to the maximum of 72% Na_2SO_4 salt rejection at 4 atm applied pressure.

The preparation and operational conditions could have impressive effects on membrane performance. The response surface methodology (RSM) method is a statistical and mathematical method that can examine the interactions of different factors at different levels simultaneously and thus can overcome the deficiencies of the traditional conventional methods [19]. This method was used to analyze a series of experiments performed to remove heavy metal from a polyamide nanofiltration membrane to produce potable water [20]. In another study, RSM was employed to optimize preparation conditions of PVDF/TiO_2 mixed matrix membrane for application as ultra filter material. After identification of the polymer and TiO_2 concentration, and membrane casting thickness as the governing parameters in membrane fouling, a three-factor CCD combined with RSM was used to optimize the membrane fabrication parameters for maximizing the permeation flux and rejection. Optimization process using CCD provides a reliable means to prepare membrane with desired performance [21]. In another study, RSM was used to extend predictive models for simulation and optimization of sodium chloride aqueous solutions as model solutions in RO desalination method [22]. RSM has also been employed by researchers to optimize preparation conditions of hybrid pervaporation membranes. The quadratic effects and interactions of the variables on the selectivity and total flux of these membranes were studied by the analysis of variance (ANOVA). The results demonstrated that the silicate loading and polymer concentration were the main parameters affecting on the hybrid membrane's selectivity and total flux [19]. In a recent work on CA/GO nanocomposite membranes, the salt rejection and permeability performances at a constant pressure of 20 atm and constant salinity of 2000 ppm NaCl solution were studied and the influence of 0.0001–0.01 wt% of GO on the morphology and pore size of membranes were investigated [23]. CA/GO nanocomposite membrane has been studied before for seawater desalination [24]. It is shown that 1 wt% GO improve mechanical strength and thermal stability simultaneously with salt rejection of CA membrane and the morphology of pores changed from finger-like to sponge-like shape. In another investigation [25], it is shown that the presence of GO in cellulose triacetate reverse osmosis membrane leads to higher permeate flux and improved mechanical property.

In this study, mixed matrix membranes were prepared and the effect of various concentrations of GO in the casting solution of CA on the morphology and desalination performance of membranes were investigated. GO concentration, feed salinity and applied pressure were selected as significant parameters in controlling the membrane performance. The specific objectives of the present study were to apply a three-factor CCD combined with RSM to optimize main parameters for maximizing the permeation flux and salt rejection. GO was incorporated into CA matrix using the phase inversion method. The behavior of the prepared membranes was evaluated using cross-flow filtration of NaCl solution. Scanning electron microscopy (SEM) studies were performed to investigate the morphology of the mixed matrix membrane. CA/GO membranes were produced with various contents of 0.0025, 0.00625 and 0.01 wt.%. The performances of these GO-blend membranes were compared with that of a blank CA membrane. Since cross-flow pattern is usually used in industrial nanofiltration modules, we also used this pattern in our experimental works to commercialize cellulose acetate membranes.

2. Experimental

2.1. Materials and chemicals

All chemicals used in the experiments were of research grade. Cellulose acetate with an average molecular weight of 30,000 $g \cdot mol^{-1}$, and 39.8 wt.% acetyl content (Sigma-Aldrich) was used as the polymer matrix after drying overnight at 90°C. Acetone, formamide and sodium chloride were supplied from Merck, Germany. Isopropanol (99.5%) (Sigma-Aldrich) and *n*-hexane (99%) (CARLO ERBA) were used as exchange solvents. Graphene oxide nanoplatelets with the thickness of ~3.4–7 nm, lateral dimension of 10–50 μm, carbon purity of ~99%, surface area (BET) of 100–300 m^2/g and bulk density of 1 gr/cc (US Research Nanomaterials, Inc.) were used in this work.

2.2. Mixed matrix membrane (CA/GO) fabrication

The CA/GO membranes were synthesized via phase inversion method. CA was dried in vacuum at 90°C for 24 h before use. The blank CA and CA/GO membranes were prepared by a weight ratio of 25:75 for polymer to solvent. The polymeric solution was prepared by adding cellulose acetate CA (5 g) to acetone (11.5 mL) and formamide (5.3 mL) followed by continuous magnetic stirring for 12 h. The desired amounts of GO were dispersed in acetone (6 mL) and sonicated for 30 min in an Elmasonic P30SE ultrasound bath. The graphene oxide dispersed in acetone was gradually added to the cellulose acetate solution, under controlled stirring conditions to avoid bubbles. The mixture was kept stirring for 15 min at room temperature, and then sonicated for 2 min more to obtain a homogeneous dispersion. The solutions of CA/GO composite films were cast onto a clean glass plate with 250 µm thicknesses using casting knife. The membranes were immediately dipped into a 15°C di-ionized water bath up to one hour and then 10 min at 90°C. Then, the membranes were immersed in isopropanol and then *n*-hexane, and finally dried by dry air to be ready for taking SEM images [26]. The pre-selection of the range of GO percentage was primarily based on the previous research works [8,23,27]. The accuracy of the selected range is approved by a) the deficiency in the membrane performance and b) observing the macro-voids and tortuous pathway in the membrane as is seen in the SEM image (Fig. 6e).

2.3. Membrane characterization and testing

The GO content in the CA/GO blend membranes were 0.0025; 0.00625; 0.01 and 0.0125 wt.% based on the weight of CA. The blank CA membranes were prepared as reference samples.

The morphologies of the cross-section and surface of the MMMs were studied by a scanning electron microscope (SEM Vega TESCAN, Czech Republic). To evaluate the hydrophilicity of membrane surfaces, a contact angle analyzer (DSA 100, Kruss, Germany) was used. Contact angle values were investigated by means of at least five measurements in different locations of the membrane samples via a sessile drop method at room temperature.

2.4. Desalination and permeation experiments

The performance of the synthesized nanofiltration mixed matrix membranes was evaluated by a cross-flow flat sheet setup which had three parallel pressure vessel cells with the possibility of three tests at the same condition and each one had 28 cm² effective filtration area. The scheme of the cross-flow filtration pilot plant is shown in Fig. 1. Tests were conducted at 25°C in different transmembrane pressures between 6–24 bar with different feed salinities between 1300–9700 mg/L NaCl solution. One can evaluate the salt rejection efficiency (S.R. %) of the composite membranes by calculating and comparing the electrical conductivity of feed water and permeate:

$$S.R.(\%) = \left(1 - \frac{C_p}{C_f}\right) \times 100 \quad (1)$$

where C_f represents the concentration of the salt in feed solution and C_p is the concentration of salt in the permeate

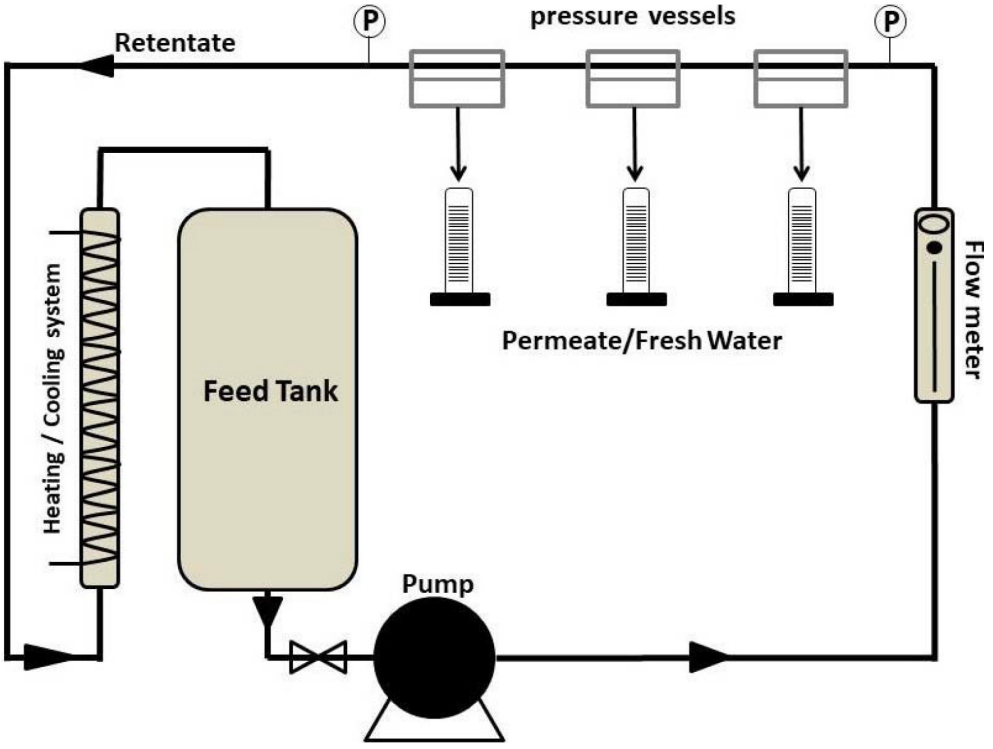

Fig. 1. The scheme of the cross-flow filtration pilot plant system used in this study.

(mg/L). Also, the following equation can be used to calculate the permeability of composite membranes as specific flux (J (L/m²h)):

$$J = \frac{V}{At} \tag{2}$$

where A, V and t are the effective area of the membrane (m^2), the volume of permeate (L) and permeation time interval (h), respectively. To report constant and reliable values for each measurement, they have been collected after 1 h stabilization time for compaction of membranes. In order to minimize errors and obtain reliable data, each experiment was repeated three times and the average values were reported.

For analysis of permeate water after each desalination test, total dissolved solids (TDSs) of the feed and desalinated water were determined using a conductance tester (EZDO TDS-5031).

2.5. Experimental design and statistical analysis

In the current study, central compositional design (CCD), a widely used form of RSM, was used to study the effect of all variables simultaneously on the performance of CA/GO mixed matrix membranes applied for desalination of NaCl aqueous solution. The number of experiments can be minimized by using design of experiments (DoE). According to the RSM, the second-order polynomial regression models can be developed to analyze the interaction between parameters. During RSM operation, the input variables must be scaled to coded levels which vary from (–1) corresponding to a minimum level, up to (+1) corresponding to a maximum level. A quadratic approximation model corresponding to the second-order equation was considered to describe the response as [28]:

$$y = b_0 + \sum_{i=1}^{k} b_i x_i + \sum_{i=1}^{k} b_{ii} x_i^2 + \sum_{1 \le i \le j}^{k} b_{ij} x_i x_j + \varepsilon \tag{3}$$

In which y is the predicted response of the process, x_i and x_j refer to the coded values of the variables (independent or control factors), b_0 is the constant coefficient and b_i, b_{ii}, b_{ij} are the linear, quadratic and second-order regression coefficients, respectively, and is the statistical error. CCD with three independent process variables (graphene oxide concentration weight ratio (X_1), feed solution salinity (X_2) and applied pressure (X_3)) and five levels (± α, ± 1, 0, where $\alpha = 2^{3/4} = 1.682$), including six replications at the central points, was used to design experiments. The variables involved in this study are summarized in Table 1. Design with 20 runs, membrane permission flux (J (L/m²·h)), and salt removal efficiency (% SR) were measured as response variables. Six replications were used at the center of the design for estimation of error sum of squares. To maximize the effects of variables on the observed responses, the experiments were randomized. The experimental design, which was computed using Minitab-18 software, along with the results are represented in Table 2. Using the same software and based on mathematical analysis of the experimental data, the contour plots were fitted to analyze the interaction between independent factors. The response surfaces were plotted for different interactions of two independent variables by keeping the value of the other variable at its central level (0). These three-dimensional surfaces could provide useful information about the behavior of the system in experimental design. It was found that interactions between the three chosen independent process variables could have significant effects on the membrane performance.

3. Results and discussion

3.1. ANOVA analysis and quadratic model

GO concentration (A), feed salinity (B), and applied pressure (C) were chosen as suggested factors to investigate their effects and interactions on membrane permeation flux and salt rejection ability. We used statistical estimators (p-value, F-value, R^2 and Adj. R^2) to measure the effectiveness of the model. To ensure a precise model, three factors should be tested: the significance of the regression model, the significance of individual model coefficients and lack-of-fit. In general, the significant factors can be classified according to P-value. The smaller the magnitude of P-value, the more significant is the coefficient terms. When the P-value is lower than 0.05, the corresponding factor will be statistically more significant, whereas it is not significant, when P-value is higher than 0.1 [29]. The results of ANOVA for the salt rejection ability and the permeate flux are given in Table 3 and Table 5, respectively. The analysis of variance showed the lowest P-value (0.000) and the highest F-values for both quadratic models. This suggests that salt rejection ability and membrane permeation flux are significant and the regression models are good predictors of experimental data. The coefficient of determination (R^2) ranges from 0 to 1 and, however, a model can fit the data with high accuracy if R^2 coefficient is at least 0.8 [30]. The R^2 coefficient for membrane salt rejection ability is 0.9745

Table 1
Coded and actual values of the parameters used in central composite design

Factor	Symbol	Actual value of coded level					Variation interval, *i*
		$-\alpha^a$	–1	0	+1	$+a^a$	
GO (wt. %)	A	0.00	0.0025	0.00625	0.01	0.0125	0.00375
Salinity (ppm)	B	1295.5	3000	5500	8000	9704.5	2500
Pressure (bar)	C	6.59	10	15	20	23.4	5

$a^a = 1.682$ (star or axial point for orthogonal CCD in the case of three independent variables).

Table 2
Design layout and response of CCD of experiments for CA/GO mixed matrix membranes for desalination of brackish water

Standard run no.	Run	Factors (controllable input variables)						Responses			
		GO content		Salinity		Pressure		Salt rejection		Flux	
		X_1	GO (%)	X_2	Cf (ppm)	X_3	P (bar)	SR (%)		J (L/(m² h))	
								*	**	*	**
1	6	1	0.01	–1	3000	1	20.00	44.1	48.80	13.0	12.98
2	8	1	0.01	1	8000	1	20.00	37.5	37.36	12.0	12.16
3	1	–1	0.0025	–1	3000	–1	10.00	72.1	76.70	4.8	4.58
4	3	–1	0.0025	1	8000	–1	10.00	49.8	47.33	5.1	5.61
5	7	–1	0.0025	1	8000	1	20.00	72.5	67.97	6.2	6.63
6	10	1.68	0.0125	0	5500	0	15.00	26.2	22.84	15.0	15.20
7	9	–1.68	0.00	0	5500	0	15.00	70.5	74.30	6.9	6.40
8	4	1	0.01	1	8000	–1	10.00	15.3	16.72	8.5	8.69
9	16	0	0.00625	0	5500	0	15.00	70.3	70.70	8.2	8.15
10	5	–1	0.0025	–1	3000	1	20.00	83.7	79.41	5.3	5.60
11	15	0	0.00625	0	5500	0	15.00	72.5	70.70	7.7	8.16
12	18	0	0.00625	0	5500	0	15.00	74.5	70.70	7.9	8.16
13	17	0	0.00625	0	5500	0	15.00	67.8	70.70	8.1	8.16
14	19	0	0.00625	0	5500	0	15.00	68.9	70.70	8.2	8.16
15	11	0	0.00625	–1.68	1296	0	15.00	74.2	71.40	7.7	8.07
16	20	0	0.00625	0	5500	0	15.00	70.3	70.70	8.8	8.16
17	12	0	0.00625	1.68	9705	0	15.00	33.8	37.05	8.9	8.24
18	14	0	0.00625	0	5500	1.68	21.40	65.4	67.78	8.0	7.59
19	2	1	0.01	–1	3000	–1	10.00	46.7	46.12	10.0	9.51
20	13	0	0.00625	0	5500	–1.68	6.59	50.1	48.17	3.7	3.81

*Experimental, **Predicted

and for membrane permeation flux is 0.9818, indicating the ability of the models in explanation of more than 97.45% and 98.18% of the data deviations and the regression models are statistically significant. The adjusted R^2 values in both models (0.9596 for membrane salt rejection ability and 0.9712 for membrane permeation flux) are close to 1, representing a high correlation between the experimental and predicted responses. As it was expected, the predicted R^2 coefficient (0.9033 for membrane salt rejection ability and 0.9374 for membrane permeation flux) was close enough to the adjusted R^2 coefficient, which shows the ability of the model for a suitable prediction.

3.2. Statistical model developed for membrane salt rejection ability

Table 3 represents the parameters affecting the membrane salt rejection performance. As seen for lack-of-fit, P-value is greater than 0.05 and F-value is equal to 3.48, implying the insignificance of lack-of-fit. First-order parameters (A: GO concentration, B: feed salinity and C: applied pressure) and quadratic effect of GO concentration (A^2), feed salinity (B^2) and applied pressure (C^2), as well as interaction effect of feed salinity and applied pressure (BC) were also shown to be significant model terms where p-value was less than 0.05. The value of P-value < 0.05 implies that regression models in the study area with a 95% confidence level are statistically significant. For each factor, the larger the F-value and the smaller the P-value, the more the significance of the term in the model. Thus, the ranking of the terms according to significance is as follows: A > B > A^2 > B^2 > C > C^2 > BC.

As seen in Table 4, by the value of R^2 (0.9745) and Adj. R^2 (0.9596) which are close to 1, it can be concluded that the empirical model of mixed matrix membrane salt rejection ability is valid and reliable. Finally, the following model was developed with the coded value of membrane salt rejection ability (SR).

$$SR = 40.4 + 2873\,GO + 0.00078\,Salt + 4.59\,Press. - 556356\,GO * GO - 0.000001\,Salt * Salt - 0.18\,Press. * Press. + 0.000359\,Salt * Press. \quad (4)$$

This model can predict the percentage of salt rejection ability in a CA/GO mixed matrix membrane within the ranges of experimental parameters.

Table 3
Analysis of variance (ANOVA) table for RSM quadratic model (response: membrane salt rejection ability)

Source	DF	Adj. SS	Adj. MS	F-value	P-value
Model	7	6657.69	951.1	65.48	0.000
Linear	3	5086.7	1695.57	116.74	0.000
GO (A)	1	3198.57	3198.57	220.22	0.000
Salt (B)	1	1423.81	1423.81	98.03	0.000
Press. (C)	1	464.32	464.32	31.97	0.000
Square	3	1409.88	469.96	32.36	0.000
GO*GO (A^2)	1	882.13	882.13	60.74	0.000
Salt*Salt (B^2)	1	489.18	489.18	33.68	0.000
Press.*Press. (C^2)	1	291.88	291.88	20.1	0.001
2-Way interaction	1	161.1	161.1	11.09	0.006
Salt*Press. (BC)	1	161.1	161.1	11.09	0.006
Error	12	174.29	14.52		
Lack-of-Fit	7	144.64	20.66	3.48	0.094
Pure Error	5	29.65	5.93		
Total	19	6831.98			

Table 4
Model summary of ANOVA and regression analysis for membrane salt rejection ability

Response model	R-Squared	Adj. R-Squared	Pred. R-Squared
Quadratic model	0.9745	0.9596	0.9033

Table 5
Analysis of variance (ANOVA) table for RSM quadratic model (response: membrane permeation flux)

Source	DF	Adj. SS	Adj. MS	F-Value	P-value
Model	7	141.44	20.2058	92.55	0
Linear	3	110.69	36.8966	169.01	0
GO (A)	1	93.44	93.4402	428.01	0
Salt (B)	1	0.038	0.0378	0.17	0.685
Press. (C)	1	17.212	17.212	78.84	0
Square	2	26.038	13.0189	59.63	0
GO*GO (A2)	1	12.694	12.6936	58.14	0
Press.*Press. (C2)	1	10.997	10.9974	50.38	0
2-Way Interaction	2	4.713	2.3563	10.79	0.002
GO*Salt (AB)	1	1.711	1.7113	7.84	0.016
GO*Press. (AC)	1	3.001	3.0012	13.75	0.003
Error	12	2.62	0.2183		
Lack-of-Fit	7	1.925	0.275	1.98	0.235
Pure Error	5	0.695	0.139		
Total	19	144.06			

3.3. Statistical model developed for membrane permeation flux

Table 5 represents that the membrane permeation flux performance was contributed by the first-order parameters (A: GO concentration and C: applied pressure) and quadratic effect of GO concentration (A^2), applied pressure (C^2), the two-level interaction of GO concentration and applied pressure (AC) and interaction effect of feed salinity and applied pressure (BC), also showed significant model term where P-value was less than 0.05. The amount of P-value <

0.05 proves that regression models in the study area with a 95% confidence level are statistically significant. For each factor, the bigger F-value and the smaller P-value result in the terms with even more significance in the model. Thus, the ranking of the terms based on significance is as follows: A > C > A^2 > C^2 > AC > AB. The lack-of-fit P-value > 0.05 and F-value of 1.98 indicate that there might have been a sufficient goodness-of-fit.

According to Table 6, the empirical model of mixed matrix membrane permeation flux is satisfactory and shows reliable validity by the values of R^2 (0.9818), Adj. R^2 (0.9712) and Pred. R^2 (0.9374). Finally, it can be said that the following model was developed with the coded value of membrane permeation flux.

$$\begin{aligned} Flux = {} & -3.55 - 351GO + 0.000329Salt + 1.063Press. \\ & +66409GO * GO - 0.03477Press. * Press. \\ & -0.0493GO * Salt + 32.67GO * Press. \end{aligned} \quad (5)$$

Pareto charts of both responses are shown in Fig. 2 and as it was expected, the pareto chart ranks the factors by significance from the largest to the smallest. This model is capable of predicting the amount of permeation flux in a CA/GO mixed matrix membrane within the ranges of experimental parameters.

3.4. Membrane performance analysis

Fig. 3 shows the three-dimensional response surface plots of membrane salt rejection (SR) versus GO% concentration, feed salinity and applied pressure, which can be used to find out the effect of the parameters on the SR response. In this research, the effect of graphene oxide on the salt rejection rate was investigated for cellulose acetate composite membranes.

By increasing the GO content in CA/GO mixed matrix membrane from 0 to 0.0026 wt.%, the total salt rejection increases slowly due to tortuous pathway provided by GO which acting as a filler to ban the uncontrolled passage of ions [31] and the decrease in the free volume between polymer molecules which is dependent on GO [32–34]. The increment in the permeate flux did not reduce salt rejection because the GO nanoplates were dispersed in the cellulose acetate matrix without any defects larger than the size of sodium or chloride ions in the membrane [8]. As GO content becomes higher than 0.0026 wt.%, the membrane performance for salt rejection becomes smaller which is due to more agglomeration of GO nanoplates. Graphene nanoplates agglomeration defects the membrane surface and causes uncontrolled passage of ion and also leads to decrement in the salt rejection based on size exclusion theory [35,36] and these macro voids provide large pathways for the water and ion molecules [8]. In consistent with other researcher's results, the addition of GO to the membranes leads to significant increase in the permeate with a reasonable loss of salt rejection [8,23,27].

Operating pressure is an important parameter in membrane desalination. By varying the transmembrane pressure from 6 to 23 atm, at first, increasing the pressure to 18 atmosphere results in the enhancement of salt rejection ability of membrane which is consistent with other groups' results [37]. At pressures higher than 18 atm, the membranes exhibit higher water flux, as predicted by solution–diffusion transport mechanism in pressurized membrane systems [38], [39]. As a result of increasing permeation flux of the flow, the salt rejection ability of membranes is decreased.

In consistency with previous results, in this study, the maximum salt rejection was also achieved for the feed solution with 3500 ppm of NaCl at 25°C [39]. As the RSM model previously showed, considering the other factors and their influence, this term is not an important factor in changing the water flux.

The three-dimensional response surface plots of membrane permeation flux versus GO% concentration, feed salinity and applied pressure are shown in Fig. 4. These plots are applicable in understanding the effect of the parameters on the flux response.

As can be seen in the SEM images (Figs. 5 and 6), 0.0025 wt.% concentration of GO has a compacting effect on the CA membrane and reduces the diffusion flux of the membrane, which complies with the results obtained from the model. By increasing the number of graphene nanoplates in the mixed matrix membrane and stabilization of

Table 6
Model summary of ANOVA and regression analysis for membrane permeation flux

Response model	R-Squared	Adj. R-Squared	Pred. R-Squared
Quadratic model	0.9818	0.9712	0.9374

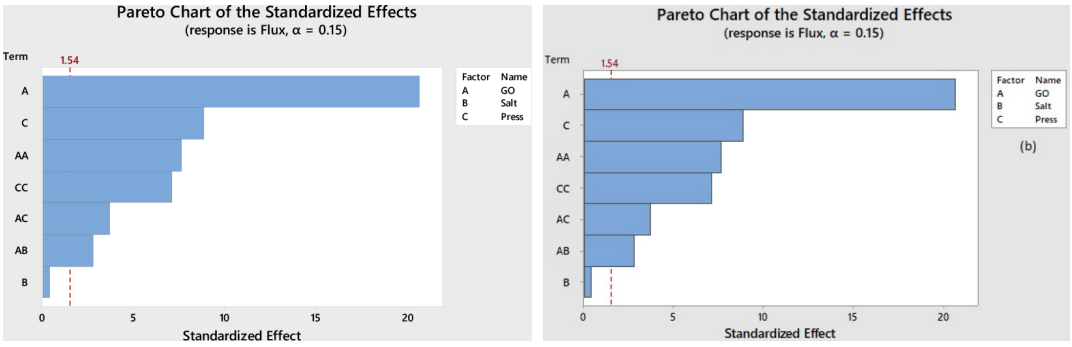

Fig. 2. Pareto charts of responses: a) salt rejection and b) permeation flux.

them, the water selective-productive capacity of the membrane increases [40]. Since graphene nanoparticles have a high specific surface area, their presence in the composite membrane structure will produce a high level of surface contact to the base polymer. This feature is likely to provide more adsorption sites for the rapid transfer of water molecules from the membrane [41,42]. The structure of the graphene nanoplates is such that they enhance the permeability of the membranes. Water flow on the surface of GO can be expressed by the surface transporting mechanism [43–48]. Variations in the physical properties and morphology are due to the presence of GO leading to enhancing hydrophilicity and as a result, increasing the permeation

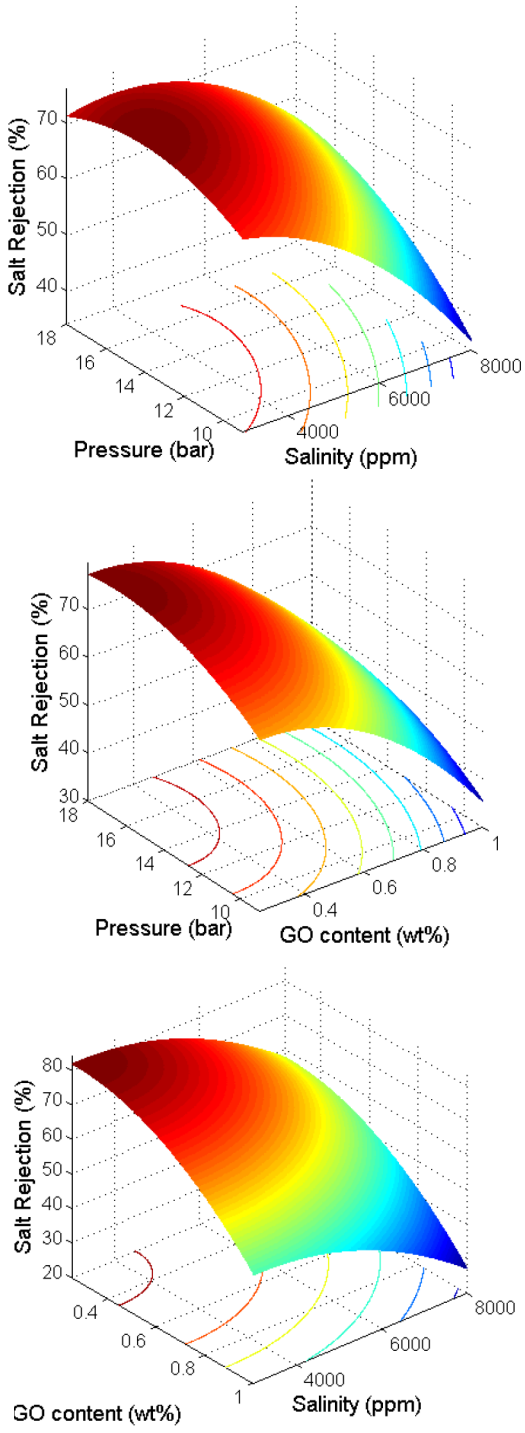

Fig. 3. Three-dimensional response surface plots of membrane salt rejection.

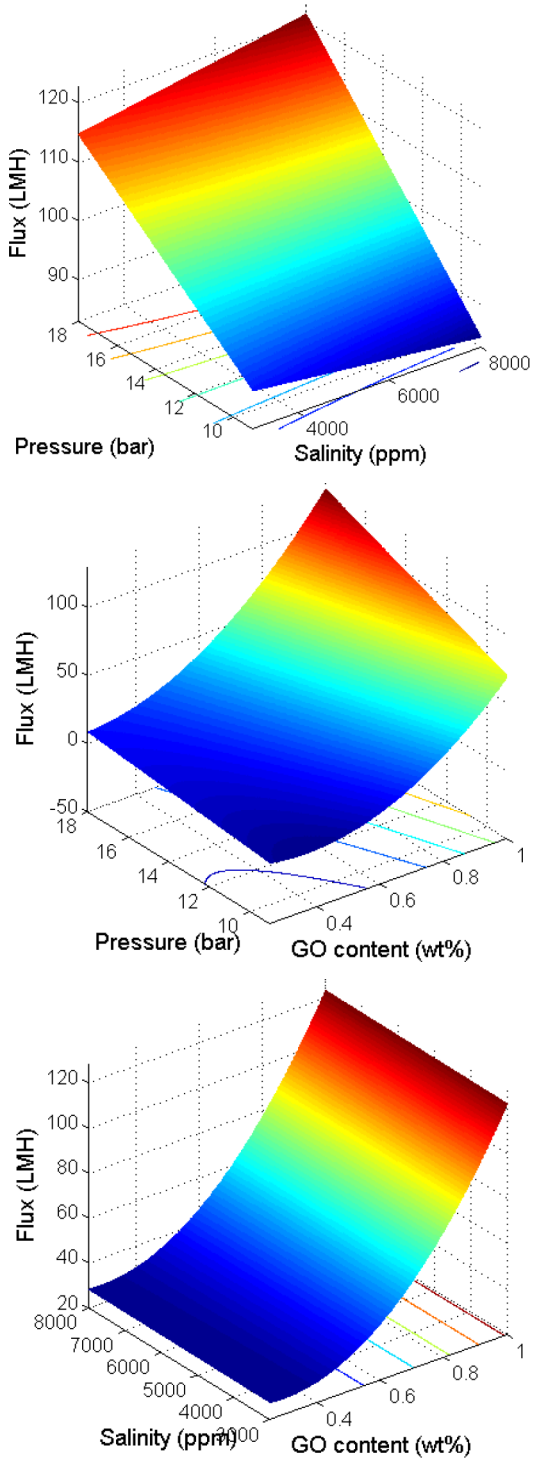

Fig. 4. Three-dimensional response surface plots of membrane permeation flux.

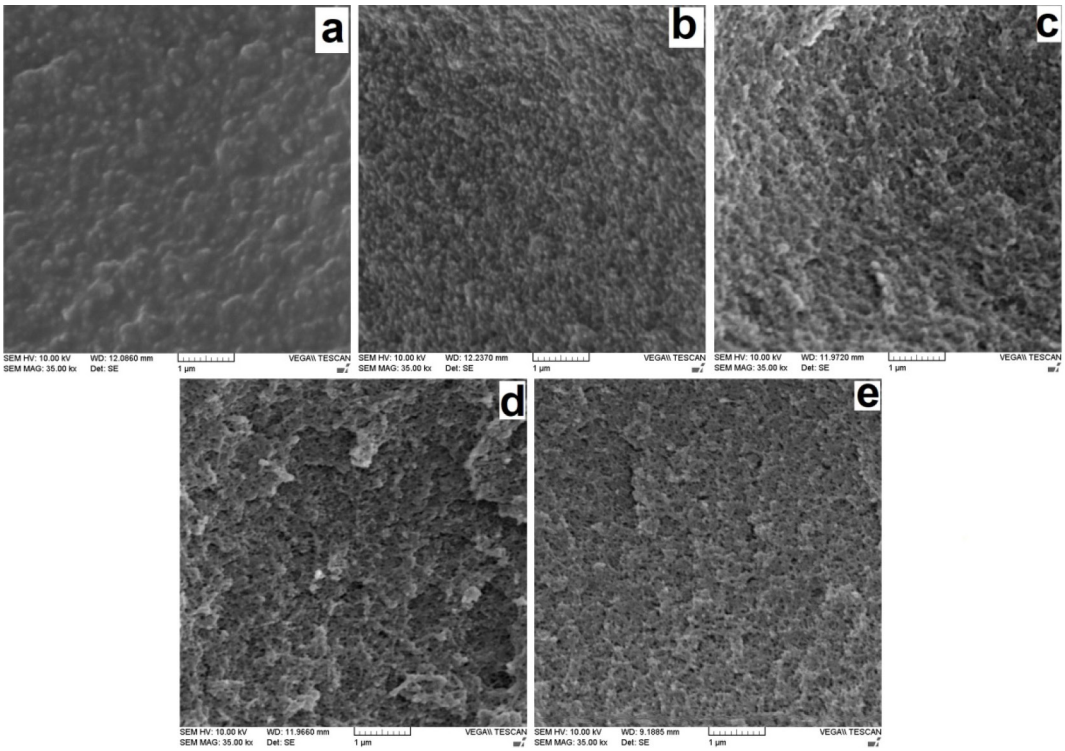

Fig. 5. Cross-section SEMs (GO content: a - 0, b - 0.0025, c - 0.00625, d - 0.01, e - 0.0125 %wt).

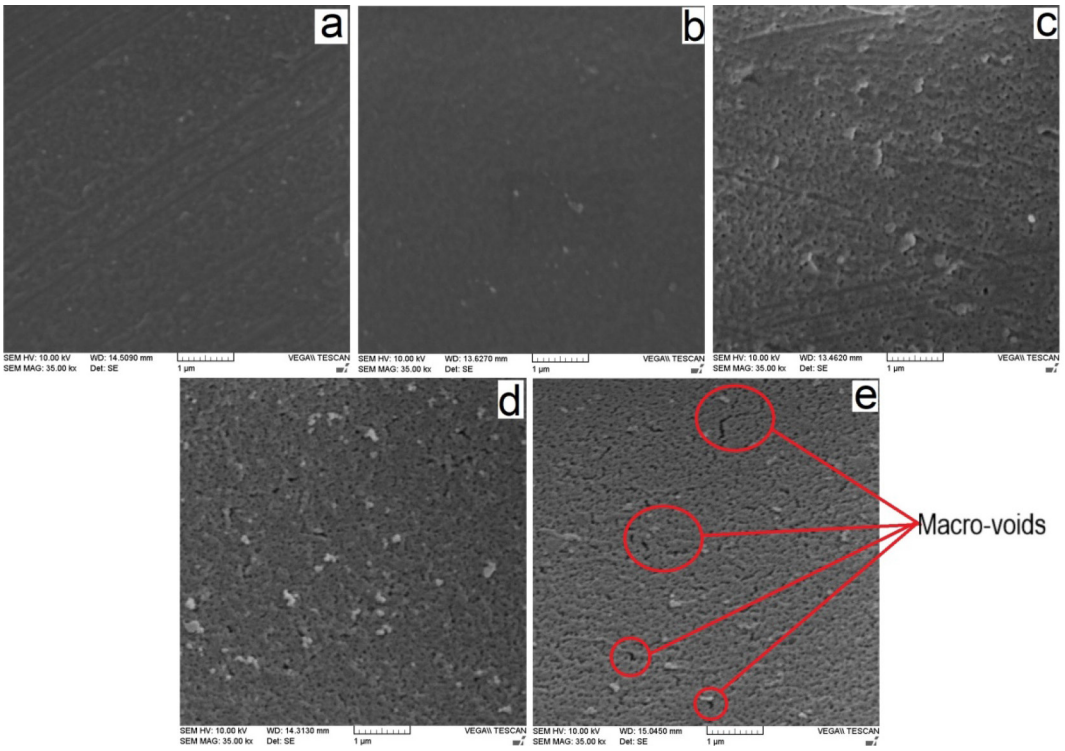

Fig. 6. Surface SEMs (GO content: a - 0, b - 0.0025, c - 0.00625, d - 0.01, e - 0.0125 %wt).

in the membrane. Hydrophilicity can be measured as the contact angle between the membrane surface and a drop of water placed on the surface of the membrane. Hydrophilic functional groups of GO, including carboxylic, hydroxyl or epoxy groups facilitate the adsorption and adhesion of water molecules on the membrane surface via hydrogen bonds between the sheets [49,50]. In addition, the membrane hydrophicity increases the ability of water to pass

through the channels of GO nanosheets in the membrane [18,51]. As previously reported, the presence of GO can boost permeability by developing special channels over the membrane via internal sub-nano-capillaries [37,52]. Table 7 shows the values of contact angle for the samples prepared in this study. The contact angle of the composite membrane is decreased from 71.5° to 47.3° by increasing the concentration of GO, suggesting an improvement in the membrane hydrophilicity.

Increasing the GO content increases the surface roughness, porosity, and pore size distribution. Rough surfaces enhance the membrane permeation flux which is consistent with the previous research [53]. According to the Cassie's law, increase in the surface roughness of hydrophilic materials leads to decrease the apparent contact angle [54]. The contact angle measurement result in this study is in agreement with other works. Shi et al. have been observed that by adding 0.01% of GO the contact angle of water on the membrane increased from 70° to 52° [23].

Table 7
Water contact angles of CA/GO mixed matrix membranes

Sample	GO (wt%)	Contact angle (°)
Pristine CA	0	71.5
CA/GO1	0.0025	62.4
CA/GO2	0.00625	58.3
CA/GO3	0.01	52.6
CA/GO4	0.0125	47.3

3.5. Verification of regression model on diagnostic plot

The normal probability plot versus residual is shown in Fig. 7. This diagnostic chart is used to determine the remaining analysis of the response surface design. In this tool, when the remnants are close to a straight line, the errors are independent of each other and are distributed normally and therefore, approve the efficiency of least square fitting. Since many residues are located near the straight line and distributed normally, it can be concluded that the experimental results are not abnormal. The plot of the predicted values versus the actual values of the responses is illustrated in Fig. 8 and the model's goodness was examined by the correlation coefficient (R^2). As shown in this figure, the proper distribution of data along the diagonal line indicates that the empirical models have a good agreement with the experimental data. Therefore, all of these cases imply that the empirical models obtained for prediction of the mem-

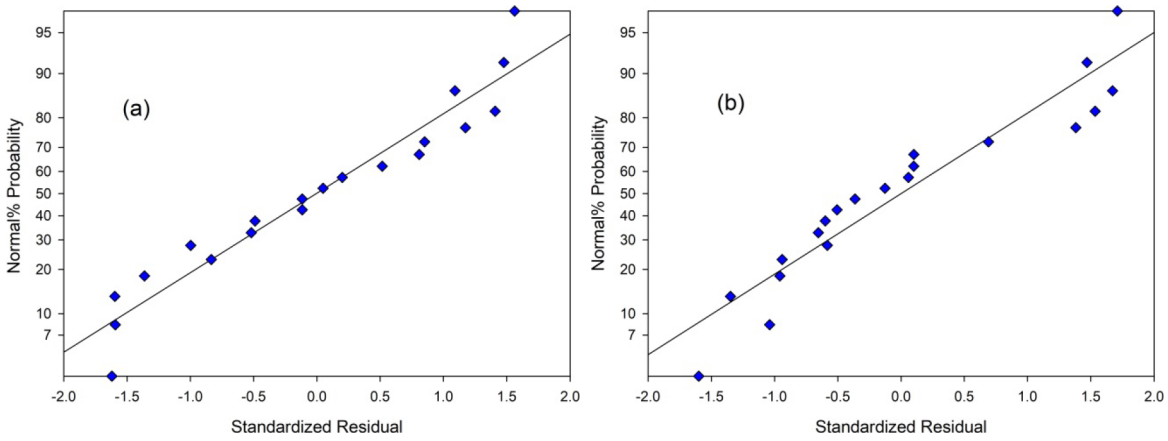

Fig. 7. Normal probability versus residual plots for: a) salt rejection ability and b) permeation flux.

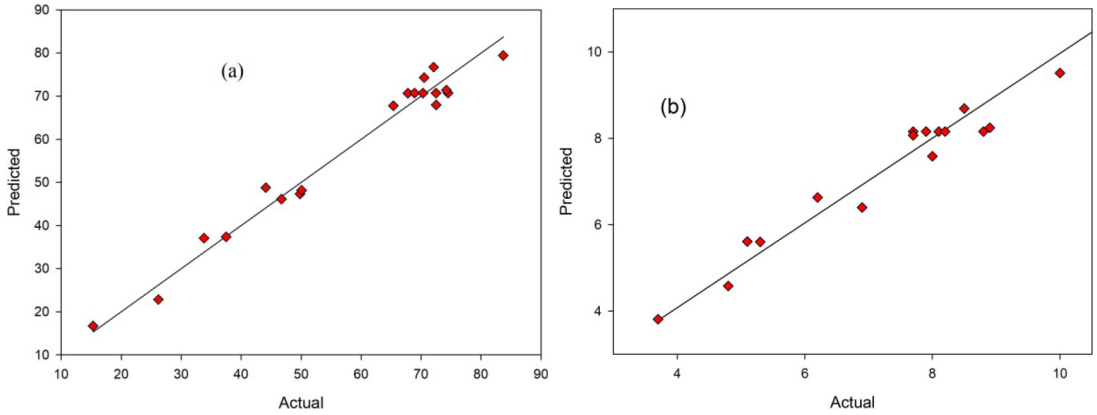

Fig. 8. Predicted values versus the actual values plots for: a) salt rejection ability and b) permeation flux.

brane functionality are reliable. The interaction and contour plots of salt rejection and permeation flux are shown in Figs. 9 and 10.

3.6. Optimization of the membrane performance

In order to utilize the highest membrane performance, all three selected parameters (GO concentration, feed salinity and applied pressure) were optimized using Minitab software simultaneously. The GO concentration of 0.009 wt%, feed salinity of 3500 ppm and applied pressure of 18 bar were calculated by central composite design approach as optimum conditions to achieve the maximum performance of CA/GO mixed matrix membrane. A membrane was prepared by using the optimum conditions, and it was demonstrated that the experimental values of 11.12 L/ m^2·h permeation flux and 58.08% salt rejection ability were in good agreement with those values predicted by CCD (11.42 L/ m^2·h and 59.53%, respectively). As a result, the optimization of membrane performance in terms of salt removal and water flux in a specific range by using CCD is a reliable approach for obtaining membranes with high desalination efficiency. The response optimization plots are shown in Fig. 11.

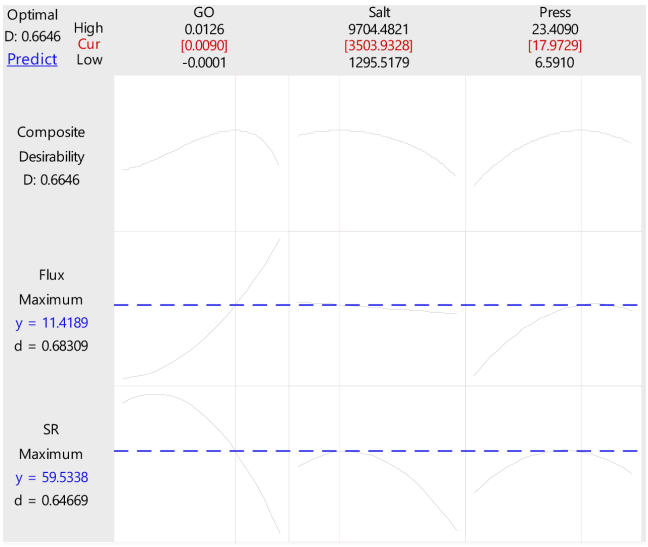

Fig. 11. Response optimization of salt rejection ability and permeation flux.

4. Conclusion

In this work, salt rejection and water flux performances in cellulose acetate reverse osmosis mixed matrix membranes containing different amounts of graphene oxide were investigated. The RSM was used to recognize and optimize the key factors affecting water permeability and salt rejection. This study led to the following conclusions:

- GO content, feed salinity and applied pressure were identified as dominant parameters in controlling the membrane performance.

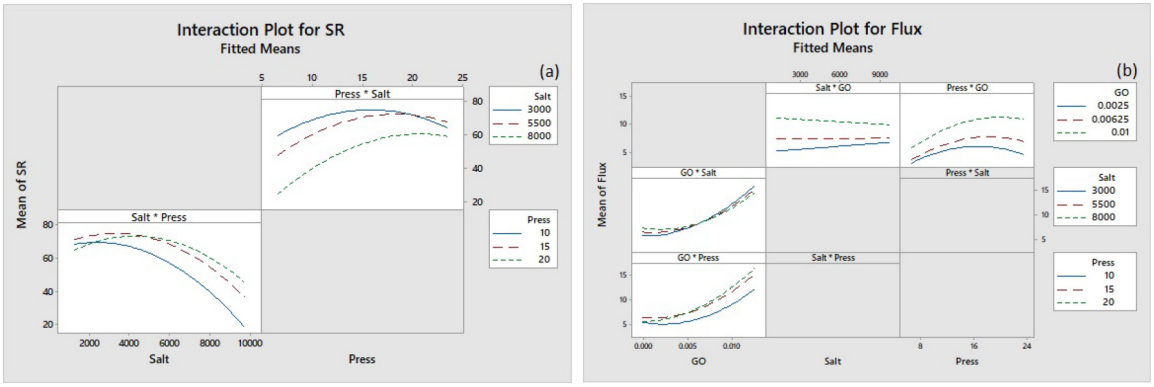

Fig. 9. Interaction plots of: a) salt rejection, and b) permeation flux responses.

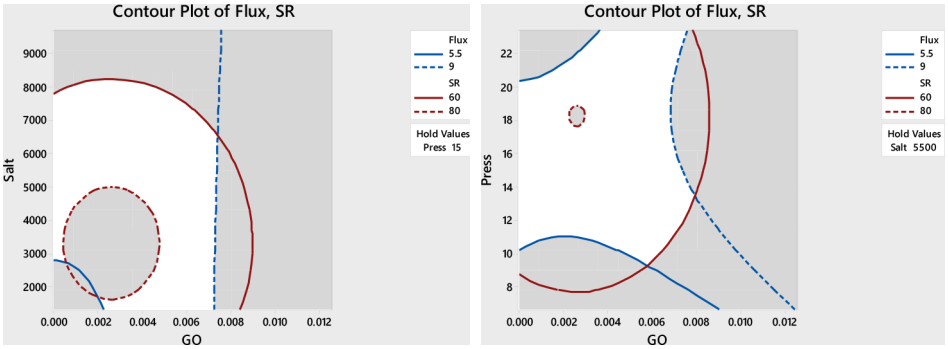

Fig. 10. Contour plots of salt rejection and permeation flux responses.

- Due to the unique characteristics of the carbon nanomaterials, GO content was found to be the major parameter affecting the membrane performance regarding to both salt rejection ability and water flux, followed by feed salinity and applied pressure.
- The presence of GO increased the hydrophilicity of the RO membrane which led to an increment in the water flux.
- To achieve high salt rejection ability and water flux as performance parameters, the selected significant parameters should be designed at 0.009%, 3500 ppm, and 18 bar for GO content, feed salinity and applied pressure, respectively.
- Good agreement between the corresponding experimental values and the optimized value predicted by RSM confirmed t.

References

[1] N. Bolong, A.F. Ismail, M.R. Salim, T. Matsuura, A review of the effects of emerging contaminants in wastewater and options for their removal, Desalination, 239 (2009) 229–246.

[2] A. Cano-Odena, M. Spilliers, T. Dedroog, K. De Grave, J. Ramon, I.F.J. Vankelecom, Optimization of cellulose acetate nanofiltration membranes for micro pollutant removal via genetic algorithms and high throughput experimentation, J. Membr. Sci., 366 (2011) 25–32.

[3] R. Haddad, E. Ferjani, M.S. Roudesli, A. Deratani, Properties of cellulose acetate nanofiltration membranes. Application to brackish water desalination, Desalination, 167 (2004) 403–409.

[4] Z. Li, J. Ren, A.G. Fane, D.F. Li, F.S. Wong, Influence of solvent on the structure and performance of cellulose acetate membranes, J. Membr. Sci., 279 (2006) 601–607.

[5] S.H. Ye, J. Watanabe, Y. Iwasaki, K. Ishihara, Novel cellulose acetate membrane blended with phospholipid polymer for hemocompatible filtration system, J. Membr. Sci., 210 (2002) 411–421.

[6] A.W. Zularisam, A.F. Ismail, M.R. Salim, M. Sakinah, H. Ozaki, The effects of natural organic matter (NOM) fractions on fouling characteristics and flux recovery of ultra filtration membranes, Desalination, 212 (2007) 191–208.

[7] T.-S. Chung, L.Y. Jiang, Y. Li, S. Kulprathipanja, Mixed matrix membranes (MMMs) comprising organic polymers with dispersed inorganic fillers for gas separation, Prog. Polym. Sci., 32 (2007) 483–507.

[8] N. Ag, Materials Chemistry A., (2014) 1750–1756. doi:10.1039/c3ta14286h.

[9] Y. Yang, H. Zhang, P. Wang, Q. Zheng, J. Li, The influence of nano-sized TiO_2 fillers on the morphologies and properties of PSF UF membrane, J. Membr. Sci., 288 (2007) 231–238.

[10] N. Rakhshan, M. Pakizeh, The effect of functionalized SiO_2 nanoparticles on the morphology and triazines separation properties of cellulose acetate membranes, J. Ind. Eng. Chem., 34 (2016) 51–60.

[11] C.H. Worthley, K.T. Constantopoulos, M. Ginic-Markovic, E. Markovic, S. Clarke, A study into the effect of POSS nanoparticles on cellulose acetate membranes, J. Membr. Sci., 431 (2013) 62–71.

[12] L.A.N. El-Din, A. El-Gendi, N. Ismail, K.A. Abed, A.I. Ahmed, Evaluation of cellulose acetate membrane with carbon nanotubes additives, J. Ind. Eng. Chem., 26 (2015) 259–264.

[13] N. El Badawi, A.R. Ramadan, A.M.K. Esawi, M. El-Morsi, Novel carbon nanotube–cellulose acetate nanocomposite membranes for water filtration applications, Desalination, 344 (2014) 79–85.

[14] H. a. Shawky, S.-R. Chae, S. Lin, M.R. Wiesner, Synthesis and characterization of a carbon nanotube/polymer nanocomposite membrane for water treatment, Desalination, 272 (2011) 46–50.

[15] W. Choi, J. Choi, J. Bang, J. Lee, Layer-by-layer assembly of graphene oxide nanosheets on polyamide membranes for durable reverse osmosis applications, ACS Appl. Mater. Interfaces, (2013) Ahead of Print, doi:10.1021/am403790s.

[16] Z. Wang, H. Yu, J. Xia, F. Zhang, F. Li, Y. Xia, Y. Li, Novel GO-blended PVDF ultra filtration membranes, Desalination, 299 (2012) 50–54.

[17] S. Zinadini, A.A. Zinatizadeh, M. Rahimi, V. Vatanpour, H. Zangeneh, Preparation of a novel anti-fouling mixed matrix PES membrane by embedding graphene oxide nanoplates, J. Membr. Sci., 453 (2014) 292–301.

[18] B.M. Ganesh, A.M. Isloor, A.F. Ismail, Enhanced hydrophilicity and salt rejection study of graphene oxide-polysulfone mixed matrix membrane, Desalination, 313 (2013) 199–207.

[19] S. Yi, Y. Su, B. Qi, Z. Su, Y. Wan, Application of response surface methodology and central composite rotatable design in optimizing the preparation conditions of vinyltriethoxysilane modified silicalite/polydimethylsiloxane hybrid pervaporation membranes, Sep. Purif. Technol., 71 (2010) 252–262.

[20] A. Maher, M. Sadeghi, A. Moheb, Heavy metal elimination from drinking water using nanofiltration membrane technology and process optimization using response surface methodology, Desalination, 352 (2014) 166–173.

[21] H.P. Ngang, A.L. Ahmad, S.C. Low, B.S. Ooi, Preparation of mixed-matrix membranes for micellar enhanced ultra filtration based on response surface methodology, Desalination, 293 (2012) 7–20.

[22] M. Khayet, C. Cojocaru, M. Essalhi, Artificial neural network modeling and response surface methodology of desalination by reverse osmosis, J. Membr. Sci., 368 (2011) 202–214.

[23] Y. Shi, C. Li, D. He, L. Shen, N. Bao, Preparation of graphene oxide–cellulose acetate nanocomposite membrane for high-flux desalination, J. Mater. Sci., 52 (2017) 13296–13306.

[24] S.M. Ghaseminezhad, M. Barikani, M. Salehirad, Development of graphene oxide-cellulose acetate nanocomposite reverse osmosis membrane for seawater desalination, Compos. Part B Eng., 161 (2019) 320–327.

[25] K. Chen, C. Xiao, Q. Huang, H. Liu, Y. Tang, Fabrication and properties of graphene oxide-embedded cellulose triacetate RO composite membrane via melting method, Desalination, 425 (2018) 175–184.

[26] I. Pinnau, Membrane separations/membrane preparation, Encycl. Sep. Sci., (2000) 1755–1764.

[27] S.S. Eslah, S. Shokrollahzadeh, O.M. Jazani, A. Samimi, Forward osmosis water desalination: Fabrication of graphene oxide-polyamide/polysulfone thin-film nanocomposite membrane with high water flux and low reverse salt diffusion, Sep. Sci. Technol., 53 (2018) 573–583.

[28] M.A. Bezerra, R.E. Santelli, E.P. Oliveira, L.S. Villar, L.A. Escaleira, Response surface methodology (RSM) as a tool for optimization in analytical chemistry, Talanta, 76 (2008) 965–977.

[29] N. Amenaghawon, K.I. Nwaru, F. a. Aisien, S.E. Ogbeide, C.O. Okieimen, Application of Box-Behnken design for the optimization of citric acid production from corn starch using Aspergillus niger., Br. Biotechnol. J., 3 (2013) 236–245.

[30] P. Qiu, M. Cui, K. Kang, B. Park, Y. Son, E. Khim, M. Jang, J. Khim, Application of Box-Behnken design with response surface methodology for modeling and optimizing ultrasonic oxidation of arsenite with H_2O_2, Cent. Eur. J. Chem., 12 (2014) 164–172.

[31] M. Safarpour, A. Khataee, V. Vatanpour, Thin film nanocomposite reverse osmosis membrane modified by reduced graphene oxide/TiO_2 with improved desalination performance, J. Membr. Sci., 489 (2015) 43–54.

[32] D.P. Suhas, A.V. Raghu, H.M. Jeong, T.M. Aminabhavi, Graphene-loaded sodium alginate nanocomposite membranes with enhanced isopropanol dehydration performance via a pervaporation technique, RSC Adv., 3 (2013) 17120.

[33] S.P. Dharupaneedi, R.V. Anjanapura, J.M. Han, T.M. Aminabhavi, Functionalized graphene sheets embedded in chitosan nanocomposite membranes for ethanol and isopropanol dehydration via pervaporation, Ind. Eng. Chem. Res., 53 (2014) 14474–14484.

[34] K.a. Mahmoud, B. Mansoor, A. Mansour, M. Khraisheh, Functional graphene nanosheets: The next generation membranes for water desalination, Desalination, 356 (2015) 208–225.
[35] Q. Wang, N. Li, B. Bolto, M. Hoang, Z. Xie, Desalination by pervaporation: A review, Desalination, 387 (2016) 46–60.
[36] C.H. Cho, K.Y. Oh, S.K. Kim, J.G. Yeo, P. Sharma, Pervaporative seawater desalination using NaA zeolite membrane: Mechanisms of high water flux and high salt rejection, J. Membr. Sci., 371 (2011) 226–238.
[37] L. He, L.F. Dumée, C. Feng, L. Velleman, R. Reis, F. She, W. Gao, L. Kong, Promoted water transport across graphene oxide-poly(amide) thin film composite membranes and their antibacterial activity, Desalination, 365 (2015) 126–135.
[38] D. Li, L. He, D. Dong, M. Forsyth, H. Wang, Preparation of silicalite-polyamide composite membranes for desalination, Asia-Pacific J. Chem. Eng., 7 (2012) 434–441.
[39] R.W. Baker, Reverse Osmosis, in: Membr. Technol. Appl., John Wiley & Sons, Ltd, Chichester, UK, 2012: pp. 207–251.
[40] Y. Gao, M. Hu, B. Mi, Membrane surface modification with TiO_2–graphene oxide for enhanced photo catalytic performance, J. Membr. Sci., 455 (2014) 349–356.
[41] D. Zhang, X. Wen, L. Shi, T. Yan, J. Zhang, Enhanced capacitive deionization of graphene/mesoporous carbon composites, Nanoscale, 4 (2012) 5440.
[42] X. Wen, D. Zhang, T. Yan, J. Zhang, L. Shi, Three-dimensional graphene-based hierarchically porous carbon composites prepared by a dual-template strategy for capacitive deionization, J. Mater. Chem. A., 1 (2013) 12334.
[43] H.J. Kim, K. Choi, Y. Baek, D.G. Kim, J. Shim, J. Yoon, J.C. Lee, High-performance reverse osmosis CNT/polyamide nanocomposite membrane by controlled inter facial interactions, ACS Appl. Mater. Interfaces, 6 (2014) 2819–2829.
[44] J.K. Holt, Fast mass transport through sub-2-nanometer carbon nanotubes, Science, 312 (2006) 1034–1037.
[45] G. Hummer, J.C. Rasaiah, J.P. Noworyta, Water conduction through the hydrophobic channel of a carbon nanotube, Nature, 414 (2001) 188–190.
[46] H.D. Lee, H.W. Kim, Y.H. Cho, H.B. Park, Experimental evidence of rapid water transport through carbon nanotubes embedded in polymeric desalination membranes, Small, 10 (2014) 2653–2660.
[47] S. Karan, S. Samitsu, X. Peng, K. Kurashima, I. Ichinose, Ultrafast viscous permeation of organic solvents through diamond-like carbon nanosheets, Science, 335 (2012) 444–447.
[48] B.J. Hinds, Aligned multi-walled carbon nanotube membranes, Science, 303 (2004) 62–65.
[49] S. Xia, L. Yao, Y. Zhao, N. Li, Y. Zheng, Preparation of graphene oxide modified polyamide thin film composite membranes with improved hydrophilicity for natural organic matter removal, Chem. Eng. J., 280 (2015) 720–727.
[50] H. Wang, L. Shi, T. Yan, J. Zhang, Q. Zhong, D. Zhang, Design of graphene-coated hollow mesoporous carbon spheres as high performance electrodes for capacitive deionization, J. Mater. Chem. A., 2 (2014) 4739–4750.
[51] M.E.A. Ali, L. Wang, X. Wang, X. Feng, Thin film composite membranes embedded with graphene oxide for water desalination, Desalination, 386 (2016) 67–76.
[52] R.R. Nair, H.A. Wu, P.N. Jayaram, I.V. Grigorieva, A.K. Geim, Unimpeded permeation of water through helium-leak-tight graphene-based membranes, Science, 335 (2012) 442–444.
[53] B. Feng, K. Xu, A. Huang, Covalent synthesis of three-dimensional graphene oxide framework (GOF) membrane for seawater desalination, Desalination, 394 (2016) 123–130.
[54] B.S. Lalia, V. Kochkodan, R. Hashaikeh, N. Hilal, A review on membrane fabrication: Structure, properties and performance relationship, Desalination, 326 (2013) 77–95.